

# Estimates of Diapycnal Mixing Using LADCP and CTD data from I8S

*Kurt L. Polzin*, Woods Hole Oceanographic Institute, Woods Hole, MA 02543 and *Eric Firing*, School of Ocean and Earth Sciences and Technology, University of Hawaii, Honolulu, Hawaii, 96822. kpolzin@whoi.edu

## Introduction

Recent fine- and microstructure measurements in the South Atlantic show that the abyssal ocean supports an enhanced internal wavefield and heightened turbulent mixing above rough topography (Polzin *et al.*, 1997). In contrast, internal waves are at background levels and mixing is weak above smooth topography. The enhanced mixing noted above rough topography appears to be sufficient to close the abyssal heat budget of the Brazil Basin. While it is tempting to argue that one can diagnose the level of mixing from bathymetric roughness, it is too soon to generalize from such limited measurements about how the abyssal heat budget of the world ocean may be closed. A more general survey to examine the issue of elevated mixing in the abyssal ocean is called for.

Numerous full-water-depth lowered ADCP (LADCP) profiles of relative velocity have been collected coincident with CTD profiles along WOCE hydrographic lines. The velocity profiles, in principle, resolve oceanic currents having vertical wavelengths from full water depth down to about 50 m. These data afford the opportunity to investigate the spatial characteristics of the finescale internal wavefield. Application of finescale parameterizations to the LADCP and CTD data permit corresponding estimates of the turbulent dissipation rate ( $\epsilon$ ) and diapycnal eddy diffusivity ( $K_\rho$ ) (Henyey *et al.* 1986, Gregg 1989, Polzin *et al.* 1995) resulting from internal wave breaking.

The rationale for applying finescale parameterizations to LADCP data is that the WOCE data set affords greater coverage of the world ocean than has been (or likely will be) obtained using dedicated fine- and microstructure instruments. Topographic variability, barotropic tidal flows and mesoscale eddy velocities are expected to be important variables in determining the energy and characteristics of the abyssal internal wavefield and, in turn, the intensity of turbulent mixing in the abyssal ocean. Lowered ADCP data have sampled abyssal waters over a wide variety of topographic and flow regimes. A global finescale internal wave survey and parameterization study utilizing the LADCP data would give great insight into which geographic/oceanographic regimes are the most important. We present below a preliminary estimate of diapycnal mixing along I8S, which crosses the Antarctic Circumpolar Current (ACC) in region of particularly strong eddy energy and topographic influence.

## Finescale Parameterization

Internal waves interact with each other and, on average, result in the transport of energy to smaller spatial scales. The intent of a finescale parameterization is to estimate this average energy flux in terms of the properties of the finescale internal wavefield, where finescale denotes vertical wavelengths of 10's to 100's of meters. The resulting energy flux to smaller scales is equated with the rate of dissipation of turbulent kinetic energy,  $\epsilon$ . One such parameterization is given by:

$$\epsilon = \epsilon_0 \frac{f}{f_0} \frac{N^2}{N_0^2} E^2. \quad (1)$$

where  $\epsilon_0 = 7.8 \times 10^{10}$  W/kg,  $f$  is the Coriolis parameter,  $f_0$  corresponds to  $30^\circ$  latitude,  $N$  is the buoyancy

frequency with  $N_0 = 3$  cph, and  $E$  is the average shear spectral density (normalized to the GM76 [Garrett and Munk, 1975, as modified by Cairns and Williams, 1976] model, i.e.  $E = 1$  for GM) for vertical wavenumbers (m) smaller than a cutoff value,  $m_c$ , defined as

$$\int_0^{m_c} S_z dm = 0.7N^2, \quad (2)$$

with  $S_z$  the vertical wavenumber shear spectral density. The diapycnal diffusivity is given by

$$K_\rho = \Gamma \frac{\epsilon}{N^2} = 0.07 \times 10^{-4} \frac{f}{f_0} E^2 \text{m}^2 \text{s}^{-1}, \quad (3)$$

where the mixing efficiency  $\Gamma = 0.25$ .

Equations (1) and (3) are simplified versions of a parameterization presented in Polzin *et al.* (1995), which accurately predicts the dissipation rate to within a factor of  $\pm 2$  for both GM and non-GM internal wavefields. The nature of the simplification is that the frequency content of the internal wavefield has been assumed to be adequately represented by the GM model. As a result, diffusivity results presented below maybe biased high by as much as a factor of three if the wavefield is more inertial than GM due to wave/mean flow interactions producing critical layers.

Note also that the LADCP does not, in general, resolve the bandwidth of vertical wavenumber space ( $0 < m < m_c$ ) required by the parameterization. The cutoff value  $m_c$  corresponds to 10 meter vertical wavelengths for the GM spectrum. Wavelengths greater than 100 m appear to be unaffected by the spatial averaging inherent in the LADCP system while motions having wavelengths smaller than 50 m are damped and noise begins to dominate. In addition, there are possible errors induced by the beam separation for vertical wavelengths smaller than 100 m. We are currently conducting an intercomparison study between LADCP and expendable current profiler (XCP) velocity profiles in order to define the transfer function and noise characteristics of the LADCP. In this preliminary study, the spectral level parameter in the model ( $E$ ) was estimated by comparing the average spectral density at vertical wavelengths larger than 100 m with the spectral density in the GM76 model. While this methodology is clearly an approximation given the above description of  $E$ , the large values of  $K_\rho$  inferred below result from large spectral levels which in turn imply relatively large cutoff wavelengths ( $1/m_c > 50\text{m}$ ). As the observed spectra are typically white, we believe the resulting uncertainty in large diffusivity ( $K_\rho > 1 \times 10^{-4} \text{ m}^2 \text{ s}^{-1}$ ) estimates for any given depth bin to be  $\pm$  a factor of three with a possible bias of a factor of three.

## Results

Preliminary estimates of diapycnal diffusivity (3) were made using LADCP and CTD data from the I8S section. That section extends from  $30^\circ$  S,  $90^\circ$  E on the Broken Plateau to  $64^\circ$  S,  $82^\circ$  E south of the Kerguelen Plateau, Figure 1. Two groups of 12 profiles centered about  $35^\circ$  S and  $55^\circ$  S were examined. The  $35^\circ$  S stations are within the subtropical gyre of the Indian Ocean and the  $55^\circ$  S stations are poleward of the Antarctic Polar Front. The northernmost profile of the first group and the southernmost profile of the second are adjacent to, but not on, the sloping flanks of ridges which rise above 1500 m depth.

At  $35^\circ$  S the shear spectra are within a factor of two of GM levels to 3000 m and exhibit significant enhancement at depth. The model estimate of the vertical diffusivity is less than  $0.2 \times 10^{-4} \text{ m}^2 \text{ s}^{-1}$  for depths shallower than 3000 m, Figure 2, and approaches  $1 \times 10^{-4} \text{ m}^2 \text{ s}^{-1}$  at the bottom. The results from  $55^\circ$  S, while not unanticipated, are quite remarkable, Figure 2. Below 1000 m, the average vertical diffusivity is  $4.4 \times 10^{-4} \text{ m}^2 \text{ s}^{-1}$ , forty times larger than the estimate for a GM wavefield. The enhancement decays towards GM levels above 1000 m. The enhanced diffusivity corresponds to a factor of 5-7 enhancement of the shear spectral levels above the GM model. Depth integrated dissipation rates are 4.6 and 0.95  $\text{mW/m}^2$  for 55 and 35S, respectively. The corresponding value for the GM wavefield is 0.8  $\text{mW/m}^2$ .

## Discussion

We believe the inference of large depth-averaged diffusivities within the ACC to be robust for the following reasons. First, there was an obvious signature of vertical phase propagation in the depth range 1600–3850 m: The clockwise spectra were on average a factor of three larger than the counter-clockwise spectra. Clockwise phase rotation with depth of the velocity (or shear) vector implies upward energy propagation in the southern hemisphere. This signature implies the parameterization estimates are not dominated by noise. Secondly, although the diffusivity may be on average 40 times the GM value, estimates of the depth integrated dissipation rate differ by only a factor of 5 between 35 and 55S. The similarity in the depth integrated dissipation rate and disparity in depth-averaged diffusivity are associated with the low depth-averaged  $N^2$  in the southern ocean. Since the depth-averaged dissipation is equal to the energy flux into the internal wavefield in a one-dimensional (vertical) balance, the heightened diffusivities inferred at 55S do not imply unreasonably large energy sources to maintain the wavefield. Third, the vertical profile of vertical diffusivity corresponds quite well with that inferred by Olbers (1989) from an inverse model of the ACC based upon the Gordon atlas.

The data suggest a much stronger bottom boundary source of internal wave energy at 55S than at 35S. In general, both internal tide and internal lee-wave generation (Bell 1976) represent possible additional energy sources for the small-scale internal wavefield. The barotropic tidal flows which one can infer from Kantha (1995) do not appear to vary significantly between 35 and 55S and thus the signal of enhanced mixing inferred at 55S is not likely to be associated with the generation of an internal tide having small vertical scales, as appears to be the case in the Brazil Basin (Polzin *et al.* 1997). Also, the small-scale bottom topography (Smith and Sandwell 1994), which is the proximate cause of enhanced mixing in the eastern portion of the Brazil Basin, does not appear to differ significantly between 35 and 55S. The big differences between these latitudes are the stratification (Figure 2) and the currents (Figure 1). The ACC and associated mesoscale eddies near 55S have strong deep velocities. Depth-averaging the LADCP profiles from 3000 m to the bottom and then calculating the rms speed for each of the two profile groups used in this study, we find 18.7 cm/s at 55S compared to only 3.6 cm/s at 35S. Our leading candidate to explain the enhanced small-scale shear field and turbulent mixing inferred from the model at 55S is the generation of internal lee-waves as the mesoscale currents flow over small horizontal scale bottom topography.

If lee-wave processes are responsible for the heightened dissipations and diapycnal diffusivities at 55S, the role of internal waves needs to be considered in the dynamics and energetics of the ACC. Depth integrated dissipation rates associated with lee-wave generation at the bottom boundary (Bell, 1975) are typically an order of magnitude greater than that produced by boundary layer stresses ( $\rho C_D U^3$  with  $C_D = 3 \times 10^{-3}$ ). This implies that, if there is significant small-scale topographic roughness, the energy within the mesoscale eddy field is dissipated by internal wave generation rather than in Ekman layers. To the degree that the eddy energy associated with baroclinic instability of the Circumpolar Current is dissipated by lee wave generation, it stands to reason that the net downward transfer of eastward momentum appears as a net upward flux of eastward momentum within the internal lee-wave field, and the dissipation of these internal waves in the interior of the fluid implies significant stress divergences at mid-depth. In an Ekman type balance, these stress divergences would support a weak ageostrophic poleward flow having a large vertical scale. Defining the strength of such a circulation begs the question of how large the net downward flux of eastward momentum associated with baroclinic instability is in relation to the zonal wind stress. In addition, a significant fraction of the meridional buoyancy flux associated with baroclinic instability may occur by diapycnal processes within the stratified interior as opposed to being accomplished via air-sea interactions (Tandon and Garrett, 1996). Finally, we wish to strike a cautionary note: The mesoscale eddy field exhibits a great deal of variability along the path of the ACC and it is not clear at this time whether the 55S diffusivity profile in Figure 2 is representative of the zonal average at that latitude.

## References

- Bell, T.H., 1975: Topographically-generated internal waves in the open ocean. *J. Geophys. Res.*, **80**, 320–327.
- Cairns, J.L. and G.O. Williams, 1976: Internal wave observations from a midwater float, 2. *J. Geophys. Res.*, **81**, 1943–1950.
- Garrett, C.J.R. and W.H. Munk, 1975: Space-time scales of internal waves: A progress report. *J. Geophys. Res.*, **80**, 291–297.
- Gregg, M.C., 1989: Scaling turbulent dissipation in the thermocline. *J. Geophys. Res.*, **94**, 9686–9698.
- Henye, F.S., J. Wright and S.M. Flatte, 1986: Energy and action flow through the internal wavefield: An eikonal approach. *J. Geophys. Res.*, **91**, 8487–8495.
- Kantha, L.H., 1995: Barotropic tides in the global oceans from a nonlinear tidal model assimilating altimetric tides, 1. Model description and results. *J. Geophys. Res.*, **100**, 25283–25308.
- Smith, W.H.F. and D. T. Sandwell, Bathymetric prediction from dense altimetry and sparse shipboard bathymetry. *J. Geophys. Res.*, **99**, 21803–21824, 1994.
- Olbers, D., 1989: Diffusion parameterizations for the climatological circulation of the North Atlantic and the Southern Ocean. Parameterization of Small-Scale Processes, Proc. 'Aha Huliko'a Hawaiiin Winter Workshop, Hawaiiin Institute of Geophysics, 181–204.
- Polzin, K.L., J.M. Toole and R.W. Schmitt, 1995: Finescale parameterizations of turbulent dissipation. *J. Phys. Oceanogr.*, **25**, 306–328.
- Polzin, K.L., J.M. Toole, J.R. Ledwell and R.W. Schmitt, 1997: Spatial variability of turbulent mixing in the abyssal ocean. *Science*, **276**, 93–96.
- Tandon, A. and C. Garrett, 1996: On a recent parameterization of mesoscale eddies. *J. Phys. Oceanogr.*, **26**, 406–411.

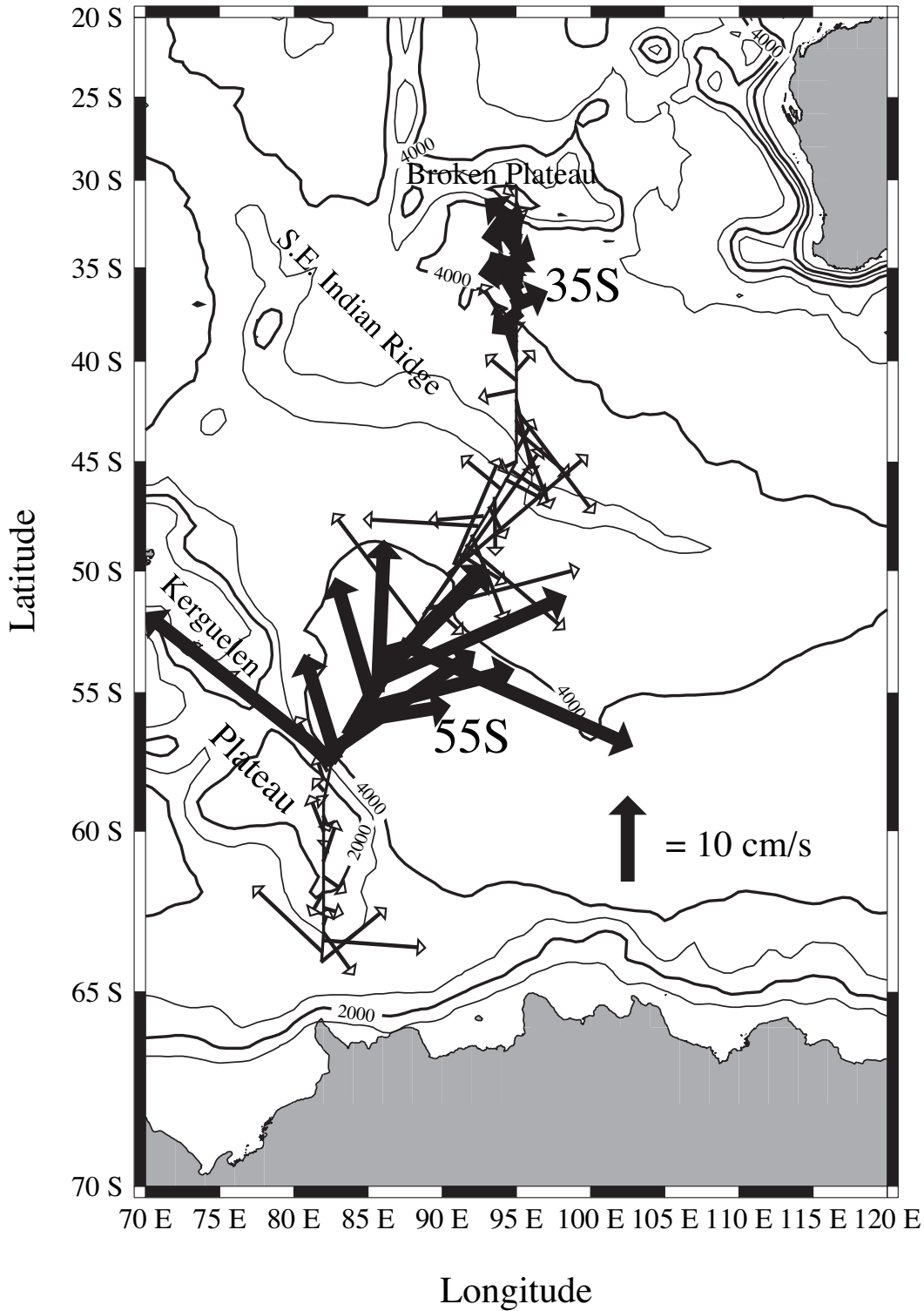


Figure 1: Bathymetry and depth-averaged current vectors along the I8S section line. The analysis focusses upon two groups of 12 profiles, one centered about 35S and the other centered about 55S. These stations are denoted with bold current vectors. The bathymetric contour interval is 1000 m, with thick contours every 2000 m.

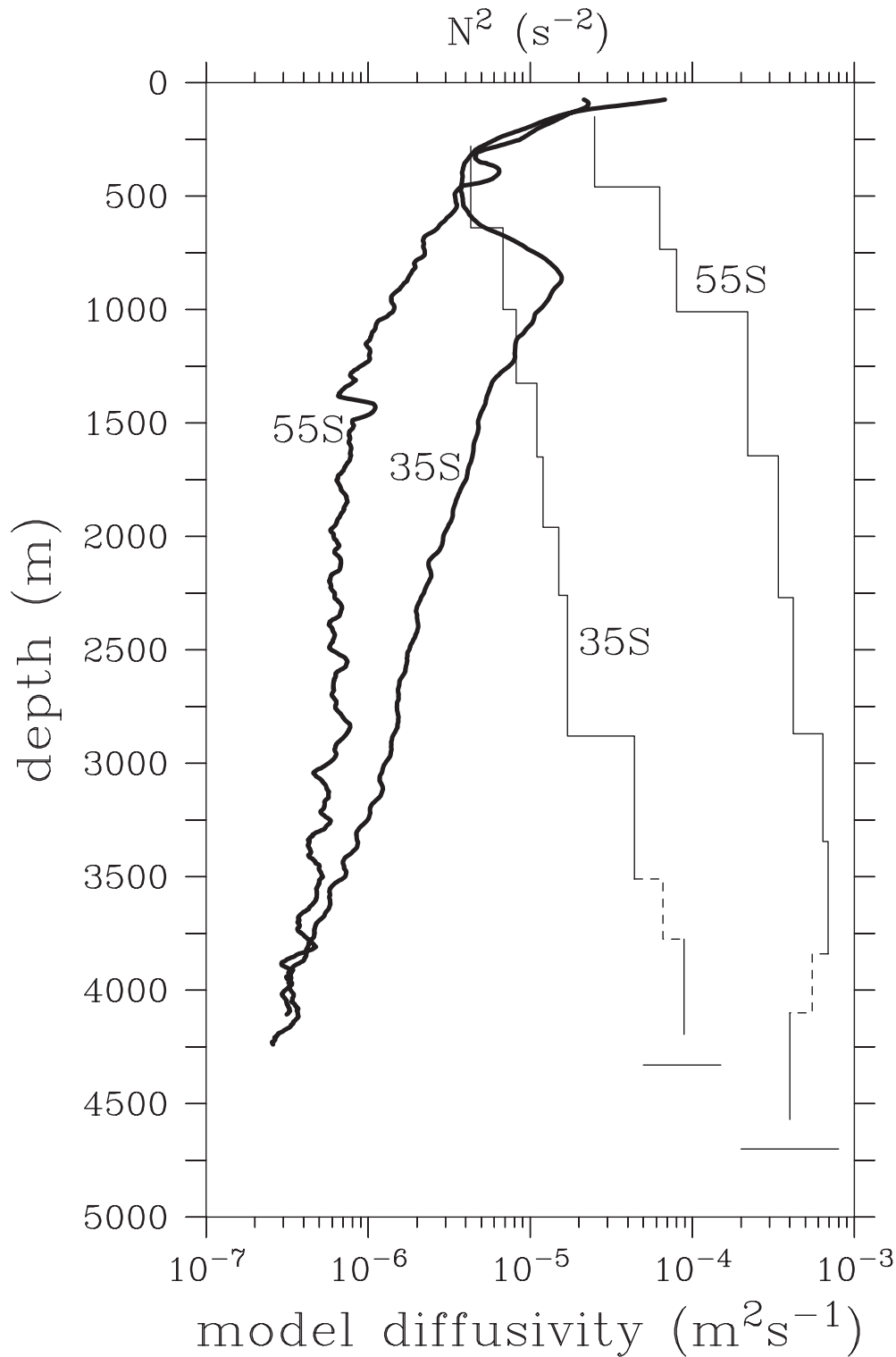


Figure 2: Vertical profiles of  $N^2$  (thick lines) and  $K_\rho$  (thin lines) for two groups of twelve stations, one at 35S and the other at 55S. The dashed lines represent regions where no data is available; the model diffusivity estimate has been interpolated through these regions. Similarly, no data is available in the bottom most 130 m of each profile. The thin horizontal lines at the bottom of the diffusivity profiles represent the average bottom depth in each case. Shear spectra for the two groups were computed using a transform interval, and averaged over depth bins of, 320 or 640 m.